ORBIT DECAY PREDICTION SENSITIVITY TO SOLAR FLUX VARIATIONS

Bo J. Naasz*
Kevin Berry†
Kenneth Schatten‡

It is well known that atmospheric density errors are the main source of uncertainty in orbit decay predictions. Perhaps less well known is the sensitivity of atmospheric density to solar activity. In this paper, we examine the sensitivity of orbit decay predictions to realistic daily variations in solar flux. We present results from analysis of orbit decay prediction for a variety of orbits, initial epochs, and predicted smooth flux profiles. For each set of initial conditions, we simulate multiple sample flux profiles with simulated daily variations, and compute the orbital re-entry date for comparison.

INTRODUCTION

In their 2005 paper on the subject, Woodburn and Lynch[1] remarked that "the computation of orbit lifetime is extremely challenging. The abundance of uncertainty makes the results of any one prediction suspect." Virtually every term in the atmospheric drag force equation has a significant uncertainty. How fast is the spacecraft really traveling with respect to the local atmosphere? What is the true spacecraft mass? What spacecraft surfaces are interacting with the atmosphere, and how? Perhaps most importantly, what is the true density of the atmosphere as the vehicle passes through it?

Accurate prediction of spacecraft orbital decay rate and eventual uncontrolled re-entry date is indeed extremely challenging. Nevertheless, important design and programmatic decisions are often influenced by these predictions. From an engineering perspective, decay rate influences the mission orbit design, propulsion system design, navigation, attitude control, etc. How high must we launch a spacecraft in order to achieve our desired mission duration? How low in order to not violate orbit debris mitigation requirements (25 years after end of mission)? How often must we perform orbit raising maneuvers? How much propellant shall we carry? How much momentum storage is required to counter aerodynamic torques? From a programmatic perspective, the decisions can be quite grave: should we perform a controlled re-entry now?

*Aerospace Engineer, NASA Goddard Space Flight Center, Flight Dynamics Analysis Branch, Code 595, Greenbelt, MD 20771, (301) 286-3819, bo.naasz_AT_nasa.gov
†Aerospace Engineer, NASA Goddard Space Flight Center, Flight Dynamics Analysis Branch, Code 595, Greenbelt, MD 20771
‡Senior Scientist, AI Solutions, Inc, Lanham, MD 20706

It is well known that atmospheric density errors are the main source of uncertainty in orbit decay predictions. Perhaps less well known is the sensitivity of atmospheric density to solar activity, or more precisely, solar extreme ultraviolet (EUV) radiation, for which the 10.7 cm radiation index ($F10.7$) is often used as a proxy. In this paper, we examine the sensitivity of orbit decay predictions to realistic daily variations in solar flux. We briefly summarize the wide range of long-term solar flux predictions, introduce our short-term flux variation modeling method, and present results from analysis of orbit decay prediction for a variety of orbits, initial epochs, and predicted 13-month smoothed solar flux profiles.

BACKGROUND

This paper stems from ongoing work by Goddard Space Flight Center (GSFC) Flight Dynamics Analysis Branch (FDAB) to properly estimate the uncontrolled re-entry date for a variety of GSFC missions. FDAB standard practice has been to periodically perform orbit decay analysis for operational missions using current initial conditions provided by Flight Dynamics Facility (FDF) ground-based Orbit Determination (OD) solutions and the most recent release of Schatten's solar flux prediction[2–4] (all available timings, with the "plus 2σ" predictions). We compute the ballistic coefficient by comparing the mean semi-major axis derived from FDF orbit determination solutions with a series of mean semi-major axis profiles computed with STK Lifetime with NOAA observed solar flux profile,[5] FDF-derived initial orbital state, and varying ballistic coefficient, as input.

Recent review of this procedure by GSFC solar physicists resulted in two suggested improvements to FDAB interpretation of solar flux prediction for orbit decay predictions. First, orbit decay predictions should use a "hybrid" method for two-solar-cycle forecasts: for Cycle 24 (this coming cycle) the polar field precursor method is best available for forecasting strength, but for Cycle 25, a conservative envelope of solar flux based on mean and variance of past cycles should be utilized. This hybrid method reflects the increased level of uncertainty in the $(n+1)^{th}$ cycle (where n is the upcoming cycle), given that the solar flux prediction of the $(n+1)^{th}$ cycle is based on measurements of the solar polar magnetic field taken during solar minimum after the n^{th} cycle. The second suggestion, that decay predictions should include and investigate the effects of short-term fluctuations in the solar flux, is the subject of this paper.

ANALYSIS APPROACH

We have already said that accurate orbit decay prediction is difficult. Actually, at present, we have little understanding of the various uncertainties in our predictions. We know that our drag force model has considerable sources of error. Most decay prediction techniques do not provide accurate models of ballistic coefficient (which is itself a kind of fudge factor commonly used to account for a large variety of effects) and its dependence on spacecraft geometry and attitude. Of greater concern is our lack of ability to accurately model atmospheric density. In their comparison of density models, Montenbruck and Gill[6] conclude that the "models have statistical inaccuracies of about 15%, and there has been no significant improvement in density models over the past two decades." Since publication of that comparison, a new release of the Mass Spectrometer Incoherent Scatter Radar (MSIS) density model, the "empirical model of choice among upper atmospheric scientists",[7] has been made. Comparisons of this new MSIS release, NRLMSISE-00, to previous MSIS and

Jacchia models in orbit determination and propagation tests[8,9] show little to no improvement for our application. Indeed, Picone, et al[7] acknowledge that even with their recent improvements to the MSIS model (including incorporation of space-bourne accelerometer data and the actual orbit decay data on which the Jacchia models are based), both MSIS and Jacchia models are sensitive to high levels of geomagnetic activity due to lack of data during geomagnetic storms.

In this work we strive to improve our understanding of the effect of short-term solar flux variations on orbit decay. Specifically, we are interested in how orbit lifetime changes as we add realistic daily flux variations to our traditional 13-month-smoothed solar flux predictions. The general analysis flow is illustrated in Figure 1. We start with three smoothed flux profile magnitudes (big, medium, and small). We then use the short-term fluctuation tool described in the next section to simulate 1000 sample flux profiles with simulated daily variations. Using the semi-analytical STK Lifetime orbit decay tool and the NRLMSISE-00 density model, we study the sensitivity of orbit decay prediction to short-term fluctuations for various orbit initial conditions and solar cycle phase and scale.

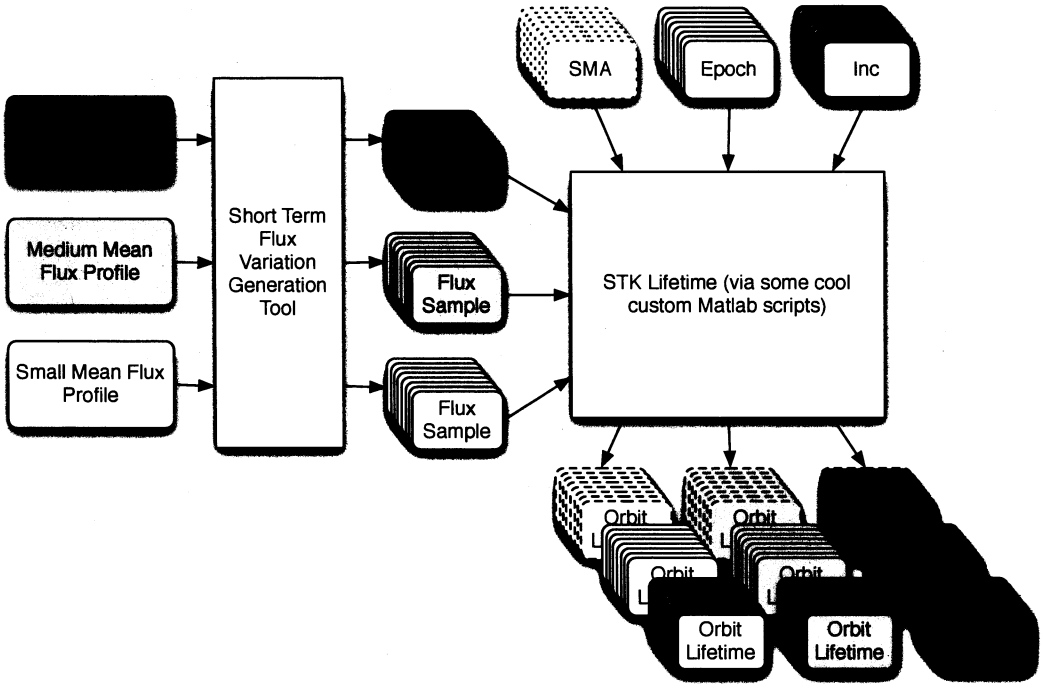

Figure 1: Analysis flow

SOLAR FLUX PREDICTION

The variability of the Sun affects spacecraft orbits. The variations of the Sun's activity may be found in discussions and Figures within texts such as Hoyt and Schatten,[10] Tandberg-Hanssen,[11] and White.[12] These authors discuss the various periodicities of the Sun and its relevance to solar-terrestrial phenomena. Through indices such as F10.7 radio flux and Ap, the indices serve as proxies for Solar EUV and geomagnetic storms, respectively. This allows these indices to serve as inputs to exospheric models. Although the solar variability exists on virtually all timescales from seconds to millennia, at present one may predict

reasonably well only on the decadal scale, although "now-casting" models - predicting on relatively short timescales (i.e. near real time) - are also making advances. Thus for most periodicities short of decadal, namely from diurnal to annual and beyond, predictions of solar activity lack a high degree of accuracy.

Despite this, variations in solar activity on various timescales are known to exist. Given the overall level of activity, even the level of variability may be estimated. It is not the amount of variability that is in question, but rather the detail. Namely, we are not able to forecast the exact time events will occur, just their overall variability. Given an overall (*smoothed* or *mean*) level of activity, the amount of activity crossing the disk of the Sun can be estimated, as it is these events that contribute towards the overall level of activity. Thus it is the purpose of this paper to provide what we shall call Monte Carlo samples of solar activity indices for use in satellite orbit forecasting.

This is undertaken through considerations of active region motions across the solar disk, their variations as they cross the Sun's disk, and their variations throughout the cycle. These variations, if well modeled, can help modelers of spacecraft orbits calculate how sensitive the orbits are to solar variability. In other words, these Monte Carlo techniques may be useful to orbit forecasters to ascertain the degree of space weather encountered by satellites in orbit by calculating how much variability the solar activity provides on timescales from days to years. We prefer this terminology, rather than simply developing a probability distribution function, as we are attempting to more closely knit our model to solar behavior rather than start from a purely statistical standpoint. Thus our approach is more physical rather than mathematical. Nevertheless, one may think in terms of probability distributions, and this may at times be helpful.

To this end we develop a solar variability model for the purpose of showing how sensitive spacecraft with differing orbital configurations, ballistic coefficients, etc. are to solar variations. We undertake this by a number of Monte-Carlo models of solar activity. We start from an assumed overall level of solar activity as input. The output from our model is a number of Monte-Carlo variations with which to compute spacecraft orbits.

Solar Flux Variation Modeling Methodology

The methodology we employ is modeled after the passage of sunspot groups (larger plage regions, and/or other names given to the centers of activity) on a variety of spatial and timescales. These regions also go by the names spots, bipolar regions, unipolar regions, plage, McMath region, Active Longitudes, etc., each with increasingly larger sizes and time periods. Figure 2 illustrates the various regions of activity, and the complexity in identifying them by name, as the regions spread out in the solar atmosphere to different amounts at various levels. This figure illustrates four views of the solar atmosphere from the photosphere (upper left) into the corona (lower right) taken by NASA's Michelson Doppler Imager (MDI) and Extreme ultraviolet Imaging Telescope (EIT) X-ray, and EUV imagers aboard the Solar and Heliospheric Observatory (SOHO). If one were to examine the Sun closely in the photosphere (the upper left panel), one would observe the entire surface mottled with activity from Ephemeral Regions (EPR) to pores (somewhat larger regions) to the sunspots we see here.

Features clearly represent an overlap of scales on the Sun, much in the same way that weather patterns vary from single clouds to larger storm systems, fronts, hurricanes, etc. Nature really provides a spectrum for which it is convenient for humans to assign specific names to the variety of scales present. Since we are not really identifying any true

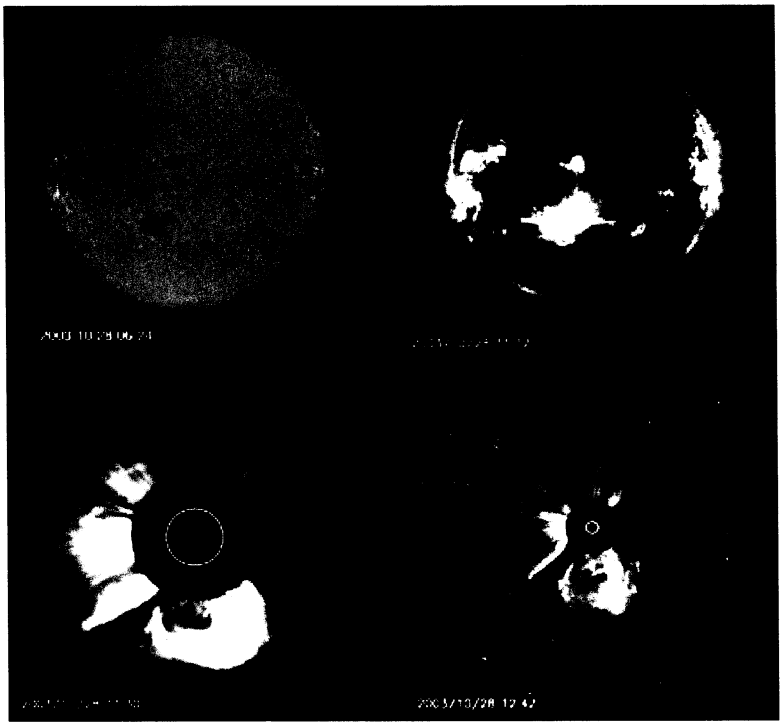

Figure 2: View of the Sun on October 28, 2003 from the photosphere (upper left), the corona in soft X-rays (upper right), and two views of the coronal blast effects associated with solar wind outbursts from the above regions. These were taken by NASA's MDI and EIT X-ray, and EUV imagers aboard SOHO.

individualized regions, we do not go through the laborious task of specifically identifying and naming each region as this serves no purpose here.

We consider spatial and temporal forms of solar variability to have variations, which are not associated with specific scales, but rather have spectral forms that vary with scale, forming a distribution pattern. Thus the various features are essentially chaotic, fractal-like objects. For time scales we choose a lower limit of a day and an upper limit of a decade for the time period these objects will fill. Two exceptions of this form we choose for specific periods in the solar activity frequency spectrum are those associated with the known decadal (11 year) and rotational (27 day) periods. These are known to be associated with the solar cycle and the rotational periods of the Sun and possess known spatial dependencies (motion across the disk, and latitudinal motion of sunspots – Spoerer's laws, and hence their reality is well established). The other periods that people have discussed often change depending on the time period considered, which is why we choose a "chaotic form." We use the term chaotic simply to mean without specific time periods, phases, etc. Chaos does not equate to random or stochastic, as the amplitudes, forms, etc., will be governed by, and bear relationship to, the overall level of solar activity. Thus the program provides a spectrum of activity similar to the Sun's.

We undertake the process of forming a chaotic underpinning to the sub-solar cycle periods as follows. We choose a variation of a waveform, given by the subroutine `wform`, which is like a wavelet transformation. It can have random amplitudes, periods and phases. We then choose variations from monthly to several years, so that this entire spectrum is filled with variations. Although alternative ways can be chosen to fulfill this, we simply

apply these forms to the original large scale input prediction.

We then choose daily variations using a portion of the same function. Here, however, we incorporate a degree of continuity to account for the fact that some fraction of active regions return a month later, due to their persistence for more than a month, as shown by autocorrelation of F10.7. There also is persistence as features rotate across the solar disk, and our basic `wform` function allows that to be considered, also. Additionally, we add a degree of "white noise" given by the subroutine function `logoran`, and the random function subroutines, which provides for a highly one-sided white noise (it can get high, but not too low). It is not known whether all the solar radio noise is real or instrumental, but the short-period (daily) noise is there in the data. There clearly is radio noise on timescales shorter than a day also, but this is as far as these programs take it. The values for Ap are taken from log normal basis; however, due to the increase in Ap in the later half of the solar cycle, we have incorporated a phase associated with location in the solar cycle to account for this. It is likely due to the presence of high-speed streams in the solar wind which enhance geomagnetic activity in the last half of the solar cycle.

Solar Flux Profiles

In this section we display a number of figures that illustrate the observed variations of the Sun's activity and some samples that illustrate how our model variations compare with these observations. To aid in understanding the Sun's variability let us examine that variability in sunspot number and solar radio flux. Figure 3 shows the daily variability of the Sun on a variety of timescales for the last 60 years. Shown are the daily variations, as well as the monthly smoothed averages, and the difference between the two. The shortest-term variations seen in the Figure are the daily variations. In addition to the long-term variations are the daily, weekly, monthly and yearly variations on all these timescales, as well as the 11 year timescale. In addition to these, there exist on the Sun secular timescales on the order of centuries and several hundred centuries not seen here. Since the convection zone of the Sun is so deep, it has a large mass. This allows these long timescales to exist as there is a long thermal timescale - up to millions of years. The long timescales are not as remarkable as the short ones. These are associated with the thinness of the upper convection zone where the solar activity manifests itself – namely in the photosphere and corona of the Sun. Densities of these regions are comparable to that in the Earth's atmosphere. The Sun as a whole has a density of about 1/3 of that of the Earth, but because the outer 2/7 roughly is convecting, huge amounts of energy are available to drive fluctuations, making for many timescale variations. The Earth's atmosphere is just a few scale heights in depth, but even the outer convection zone of the Sun has more than 10 scale heights of depth available.

A look at Radio flux over a solar cycle is seen in Figure 4. The left plot shows actual daily variations for solar cycle #23. Daily observations range from 1996 through first half of 2007. As one can see there are spikes throughout the cycle, with most at solar maximum, but some in the decaying phase of the cycle as well. In addition there are some plateaus - increases in solar activity that occur through the various phases of solar activity. Here we see timescale of variations on the order of a day (sharp spike in solar activity). These are associated with the growth of active regions on the disk of the Sun. In addition, seen less clearly, there exist timescales on the order of a week associated with the rotation of the Sun's disk - namely solar rotation. Sharp enhancements also exist on longer timescales associated with the manner in which active regions can gradually grow and shrink.

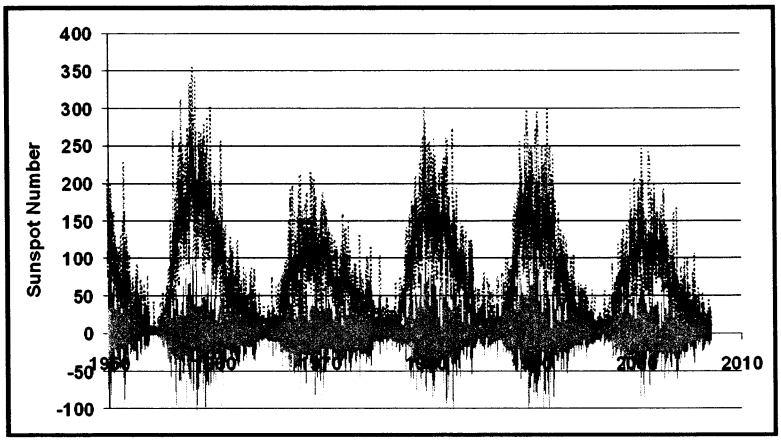

Figure 3: Historic flux profiles, including daily variations (blue), monthly smoothed (pink), and differences (light blue)

The right plot of Figure 4 provides a first look at the modeled data for one run of calculations. The amplitude of the RMS variations are in good agreement with the observed F10.7 variations. In addition, spikes exist comparable to the observations. Variations on all the apparent timescales appear to be present in approximately the observed amount.

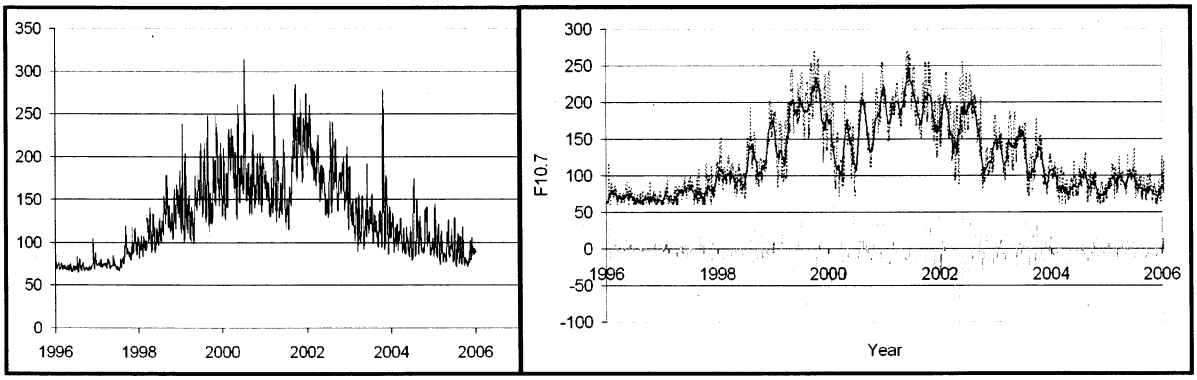

Figure 4: Actual daily variations for solar cycle #23 (left), and modeled F10.7 daily calculated data (right), daily variations in light blue (solid), smoothed values in pink (bold), raw calculations in blue (dotted))

Variations on the order of a year are seen in Figure 5. Here one notes the 27 day rotation rate variations, as well as some of the variations associated with the growth of activity centers on timescales from months to years. A rising secular trend is barely visible throughout the year. The relatively level variations throughout this period are unusual. Other time periods could show more significant changes in a similar timeframe. Additionally, in Figure 5 one notes changes from moderate activity to extremely active. There are also sharp one-day spikes that are evident throughout the solar cycle. Often these are associated with a solar flare; however, they could be associated with a coronal mass ejection and a flare might not be present.

In Figure 6 we see a sample of one year near the peak of solar activity for our cycle #23 simulation. One sees numerous samples of 27 day rotation events. We also see some periods where the 27 day periodicity is not so evident. Nevertheless the general behavior

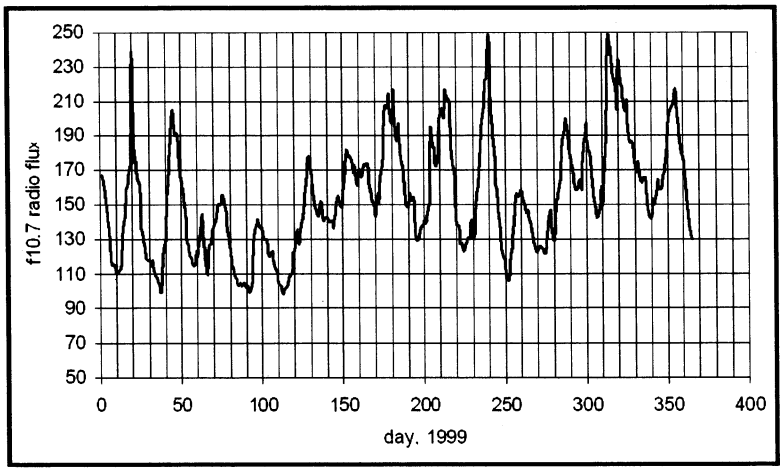

Figure 5: A year's worth (1999) of daily data shown here allows one to see the peaks within a year and the variations associated with the Sun's rotation (27 days). Actual solar rotation varies from 27 days to about 33 days (synodic) as the Sun rotates differentially.

of solar activity is seen in this run. Figure 6 also shows a sample run of 11 years of daily variations. One notes changes from moderate activity to quite active. Additionally, there are sharp one-day spikes that are evident throughout the solar cycle. Most features seen in a normal cycle (for the active time periods seen for solar cycle #23) are seen in this sample run.

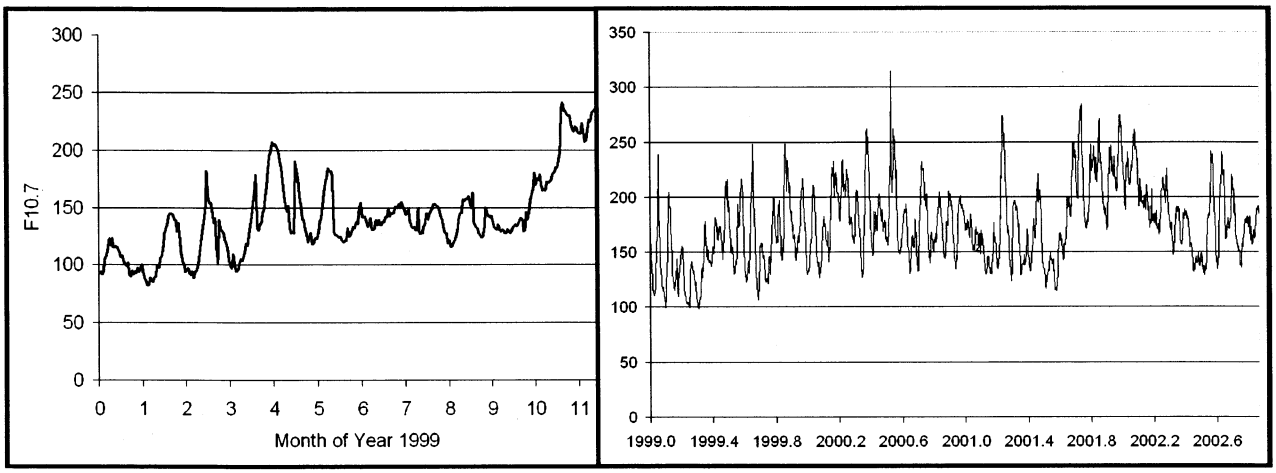

Figure 6: Going to a longer timescale, one year (left), and four years (right), 1999-2002 allows us to see some of the longer timescale variations. One can now see some of the variations associated with the growth and decay of "activity centers"

Figure 7 shows sample data for a time span from 1999-2002. This allows a longer timescale viewpoint of 27-day variations for 4 years near the cycle's peak activity. We see 27-day variations throughout the time period, although there are some periods, as there are on the Sun, when the 27-day variations are weak. At other times it is quite large. Figure 7 also shows a full 11 year solar cycle with large variations during the peak of activity, and reduced variations near solar minimum.

In Figure 8 we have a graph showing the asymmetries associated with different levels

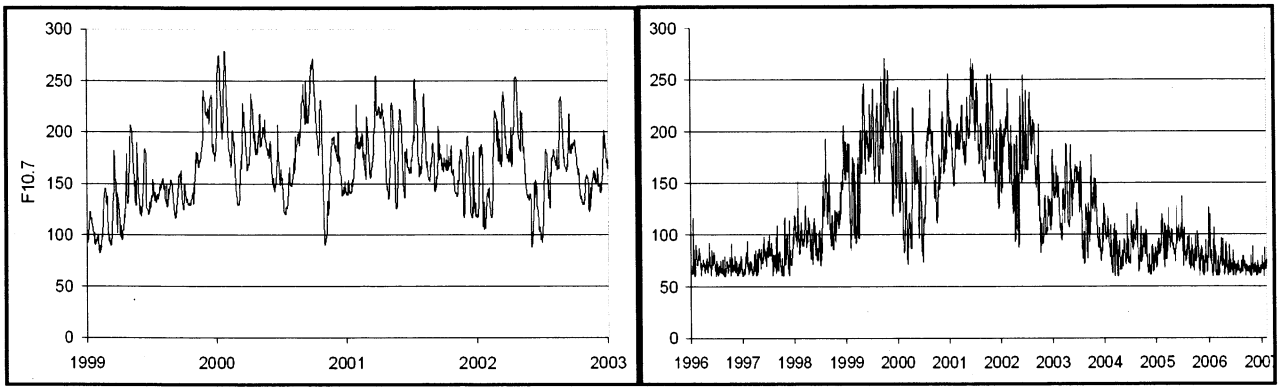

Figure 7: Four-year sample run of daily data for an active period near the peak of a sample cycle #23 model simulation (left), and eleven-year sample run of daily data for an active period near the peak of a sample cycle #23 model simulation (right).

of activity. This allows one to look at various activity periods to see the distribution of the calculated variations and ascertain the non-linear variations throughout various phases of activity. It is a useful diagnostic technique. At the low end there is an effect associated with the sharp cutoff of radio flux near the "zero level" of activity. Due to the aspect that this graph shows daily variations from the mean, there is a 45 degree slanting line that results from the sharp, flat bottom of solar activity that exists.

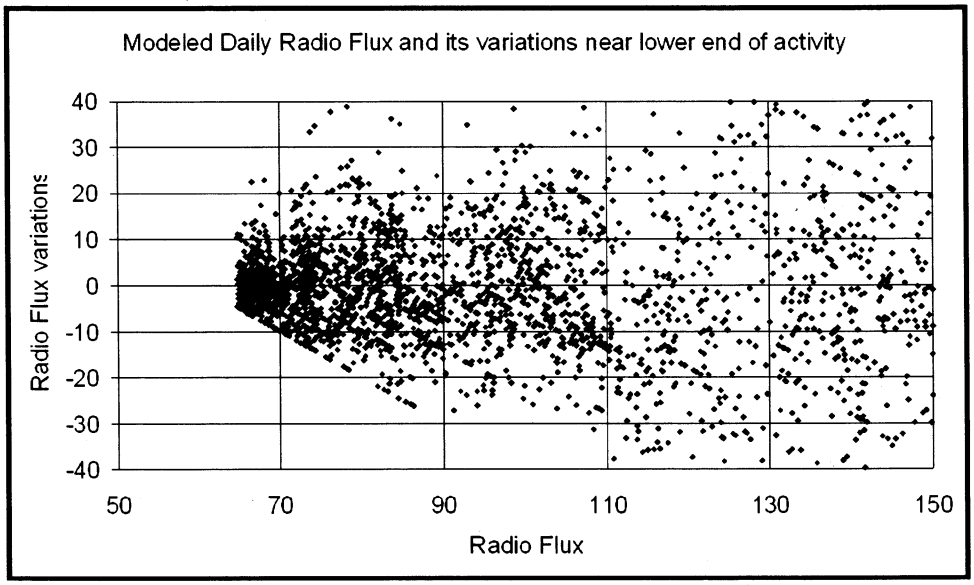

Figure 8: Modeled daily variations near the low end of solar activity

In Figure 9 we see the 11 year cycle in Ap for the past 5+ years. We see the sharp spikes associated with daily peaks in activity. The sharp one-day spikes are more evident in Ap than in F10.7. Often these are associated with a solar flare, however, they could be associated with a coronal mass ejection and a flare might not be present. The curve is roughly log normal, however, solar cycle effects also exist. Also in the figure we see the 11 year cycle in Ap and sharp spikes associated with daily peaks in activity. The two figures shown in Figure 9 show two different scales owing to the fact that the observed curve (top)

shows more than five solar cycles and the modeled curve (bottom) shows only 1 cycle. Hence the top curve has a few points above 200, extending the scale to 300. The lower curve shows a cycle filling many points between 100 and 200 for daily Ap. A solar cycle dependence is present, but not very strong, as is the case in most cycles in the top figure (the exception being cycle #19, which peaked in 1958-9 and was the largest cycle of the past 400 years).

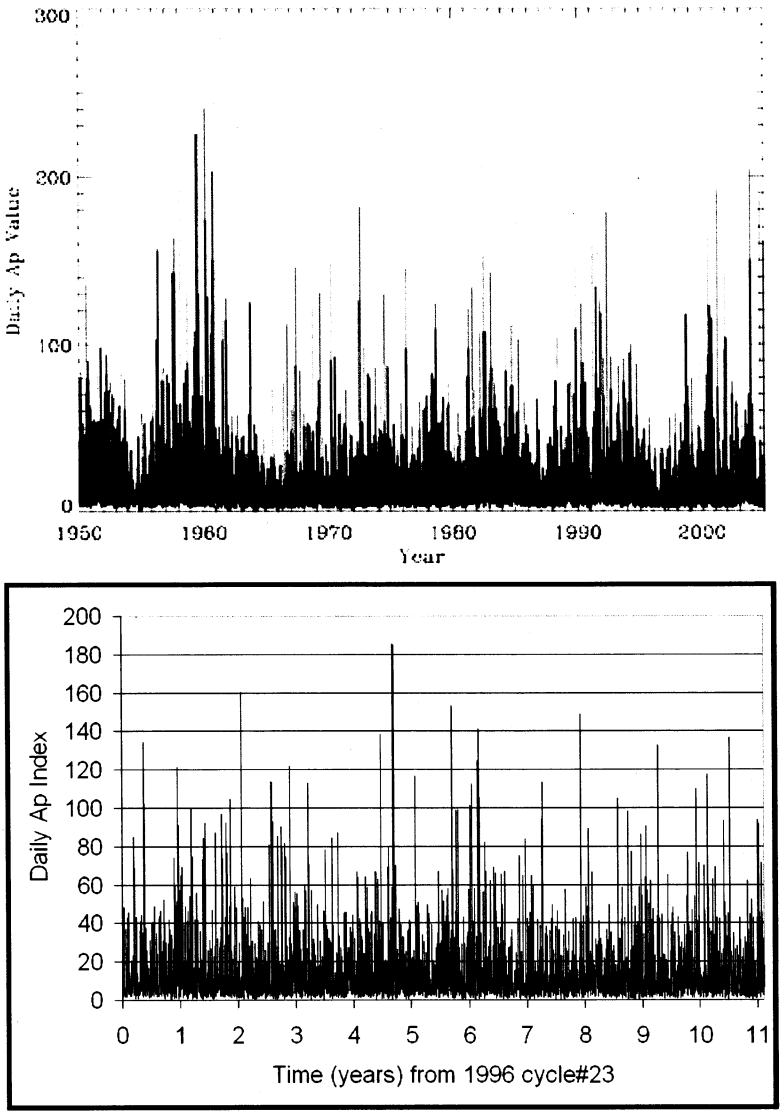

Figure 9: Observed Ap daily values for 50 + years (top) and a sample model run (bottom)

The figures shown here are simply illustrative. We have examined many runs too numerous to display. Different runs of the model show significantly different variations, just as different solar cycles with similar amplitudes have quite differing behaviors, much to the consternation of some solar physicists who prefer that each solar cycle be identical. The cycles are as different from each other as individual members of animal species, or snowflakes: no two being alike. Extensive model calculations were undertaken to develop the model parameters. Areas of future model improvement could be improving the model

for the rare events that occur during times of low solar activity. This is of particular interest, because, as we will see, it seems that the response of spacecraft in low Earth orbit (LEO) has a non-linear response owing to the exponential growth in atmospheric density, which can be sensitive to initial conditions so that early low activity solar variations may have a significantly large and possibly unexpected response to pulses of activity early in the spacecraft's orbit.

RESULTS

Having developed a method for generating random profiles of daily solar flux and A_P, we are ready to generate multiple profiles, format them for use in our orbital decay prediction tool of choice (STK Lifetime), and analyze the results. We now present these results in two sections. First we present decay results for a few orbital altitudes, and with 1000 random profiles for each of three mean flux levels. We then build on this base understanding by analyzing an extensive set of initial conditions, this time with 100 random profiles each, to reduce processing time.

For all results, we use the three input flux profiles shown in Figure 10 to generate random samples[§]. We compute statistics on the orbital lifetime (time from epoch to computed re-entry date) for each random flux sample, as well as for both the input flux profile and the mean flux profile (computed by averaging all samples at each epoch). In general, we compare the statistics on random samples to those of the mean flux profile to gauge the amount of variation in orbital lifetime induced by the short-term flux variations.

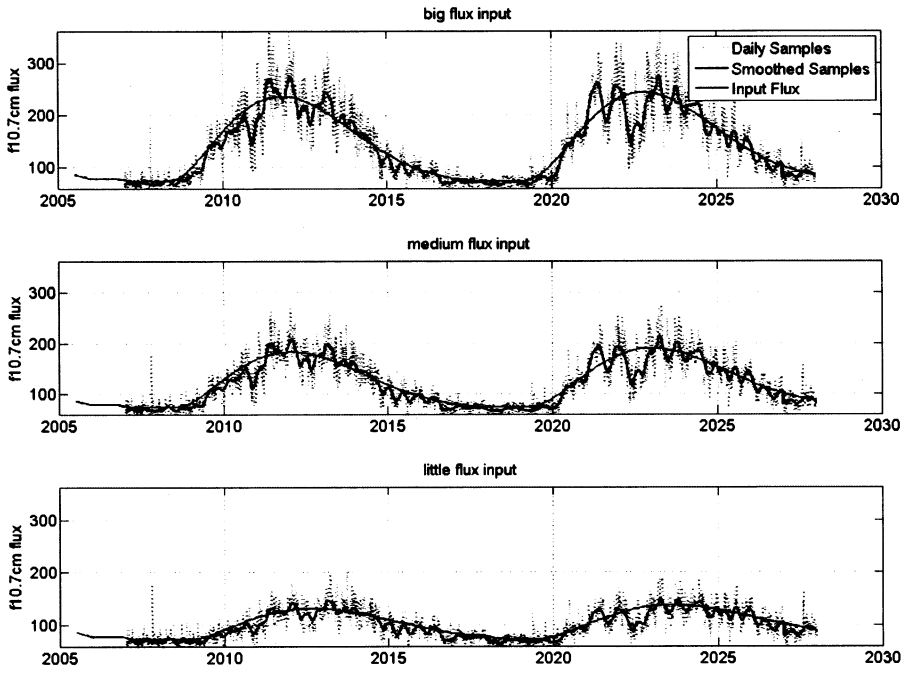

Figure 10: Sample random flux profiles generated using big, medium, and little mean-flux profiles

[§]Although each run is random for the three curves shown in Figure 10, the samples use consistent seeds and therefore have similar features

These results show the *sensitivity of orbit decay prediction* to short-term solar flux variations. None of the orbit decay "predictions" in this work are actual predictions of a real spacecraft's decay profile. The input flux profiles shown above are not real predictions. They are intended to be used only as part of this academic investigation.

1000-Flux-Sample Decay Results

Figure 11 shows orbit decay results for 1000 flux samples with initial orbit altitude of 500 km on January 1, 2007, and assuming a medium peak flux for cycle 24. The results show a mean orbit lifetime of about 6.3 years, and standard deviation of 0.3 years. Also of interest in the figure is the early re-entry of one of the sample cases, almost a year before the mean. It is not clear for this case that short-term flux need be considered. At 5% of the total

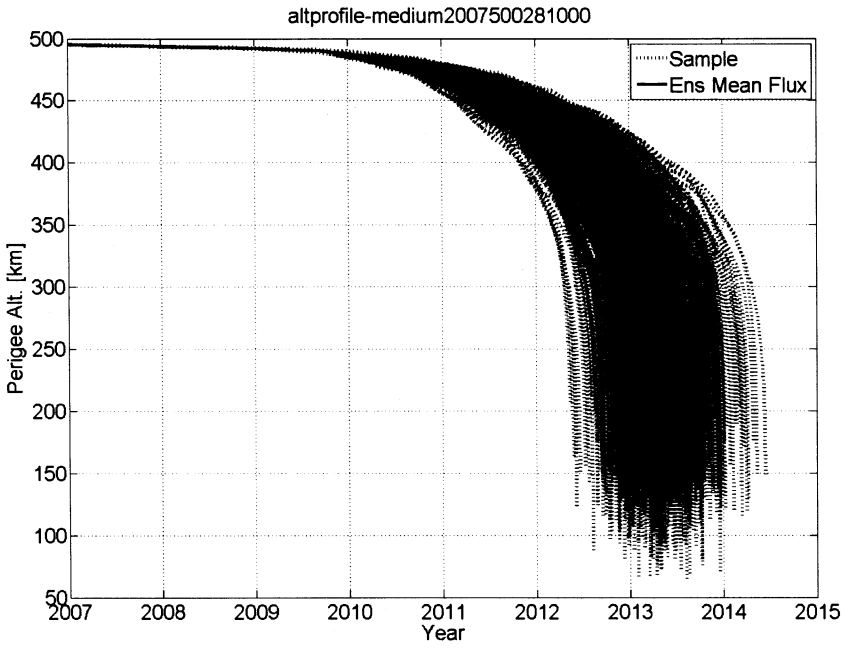

Figure 11: Perigee altitude profiles for a 1000-sample, 28° inclined, medium input flux set

lifetime, a 0.3 year 1-σ deviation may not be of concern. Even the one-in-one thousand case which re-entered a year earlier (15% of total lifetime) may not significantly influence programmatic decision-making.

Figure 12 shows a histogram of decay prediction results for a a 1000-flux-sample set with 500 km initial altitude and little, medium, and big flux input, respectively. Lines on each histogram show plus and minus 1-σ and 3-σ values, as well as the corresponding percentile values. Table 1 presents the statistics of those three runs. These cases are all very similar, with lifetime uncertainties on the order of 5%. Of interest in Figure 12 is the varying shape in the histogram as the input flux changes. Clearly these distributions are non-Gaussian. Also of interest is the group of little-input-flux cases for which re-entry occurs nearly 2 years before the mean. If these results were being used to evaluate risk of uncontrolled re-entry before a given date, clearly this grouping, and the general "fat tail" in the distribution of this set would be of interest.

These early results give us some confidence that we might ignore short-term flux results, or at the very least develop a strategy by which we assume some given error in all predictions

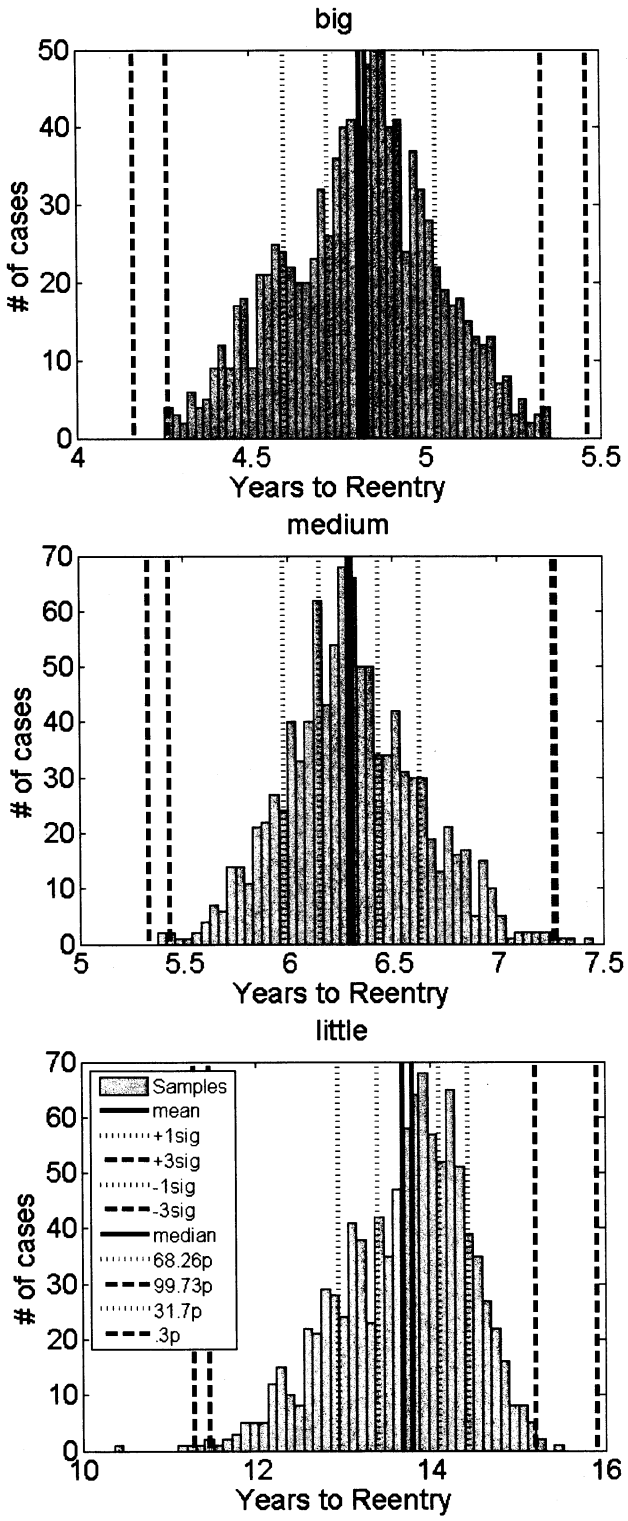

Figure 12: Orbit lifetimes for a 1000-flux-sample set with 500 km initial altitude. Input flux scales are (from top to bottom), big, medium, and little

Table 1: Lifetime statistics for three 1000-set runs with initial altitude of 500 km, and epoch near solar minimum

Flux Profile	Mean Lifetime (years)	Lifetime STD (years)	STD/Mean (%)
big	4.81	0.22	4.6
medium	6.30	0.33	5.2
little	13.68	0.74	5.3

which do not include short-term flux variations. As we shall see in the next section, not all cases are as insensitive.

Survey of Orbit Altitudes, Inclinations, and Epochs Results

We now present results with a much more dispersed set of initial orbit conditions. For each of the 3 input flux profiles, we perform orbit decay predictions for varying altitudes (300-500 km in steps of 10 km), varying inclinations (equatorial and polar), and initial epochs (2007 to 2013 in steps of 6 months). This section therefore presents results from a total of 2038 sets of 100-flux-profile-sample runs, for a total of 203,800 STK Lifetime runs.

To reduce the computation time required, we reduce the flux profile sample size to 100 for this section. Figure 13 illustrates the impact of this change on our confidence in these results. Note that while the shape of these distributions is quite different, the standard deviation changes only slightly *for this case.* We will show later that this is not always the case. Future work will include a more thorough investigation of the number of samples required to provide a high confidence in the results.

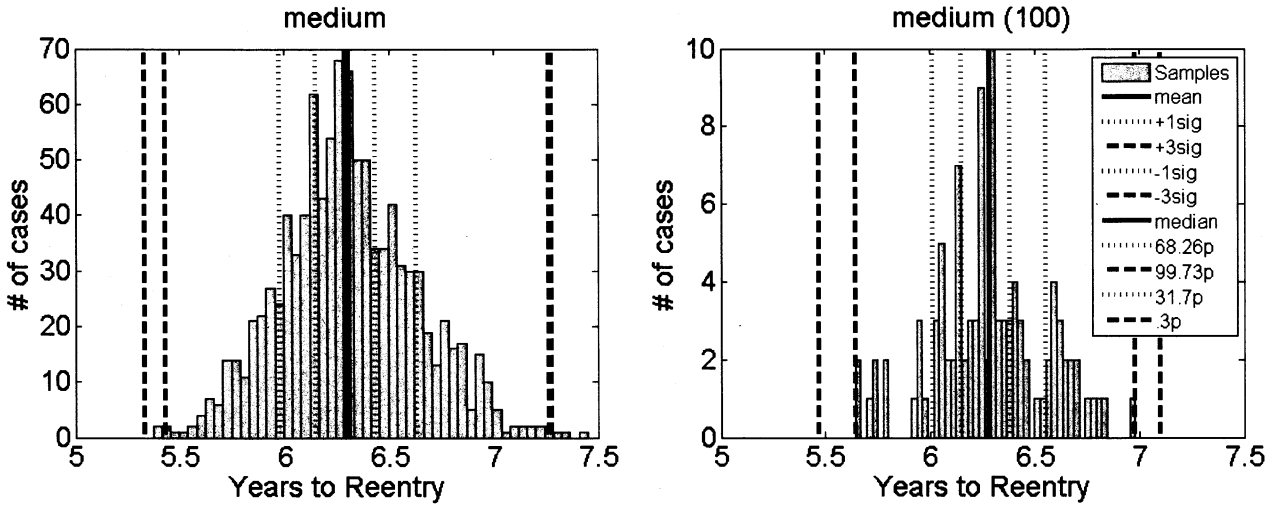

Figure 13: Comparison of 1000-sample (left) and 100-sample (right) sets, with medium input flux profile and 500 km initial altitude

Figure 14 shows several contour plots for the equatorial cases, which portray predicted lifetimes and their standard deviations as a function of initial altitude and epoch. For all three flux cases shown (ordered as big, medium, and little respectively), as one would expect, higher altitudes take longer to decay. The sensitivity to initial epoch is more subtle,

in that it causes a "wave" effect in the contour. In each plot, the left-most date is close to solar minimum while the right-most is near solar maximum. Any object with an initial altitude high enough to remain in orbit past solar maximum is likely to continue orbiting long into the next solar cycle. As we approach the wave from the left, predicted lifetimes decrease. Once we reach the wave, predicted lifetimes increase because the spacecraft now survive to fly into a period of decreasing solar flux. The most vital observation to take from these plots is in the peaks and valleys of the uncertainty contours.

In the little flux case (bottom) the interesting region is for uncertainties above 450 km. For lifetimes between 8 and 12 years the uncertainty grows up to nearly 1 year (10%), then, between 12 and 16 years the uncertainty drops closer to 1/3 year (3%), and finally, as lifetimes grow above 16 years, the uncertainty climbs up to 1.6 years (10%). A similar pattern is apparent in the big- and middle-flux cases, which both show drops in uncertainty in their upper-right corners.

The polar inclination results show no significant difference in uncertainty at this scale. Re-entry dates are earlier, as would be expected, but uncertainty contours maintain the same characteristics.

Figure 15 shows more detail into one of the cases in which the decay prediction is highly sensitive to short-term flux variations. This case demonstrates a major conclusion of the current work: in order to truly understand the uncertainty in the re-entry date of an orbiting object, we must perform Monte-Carlo analysis for that object. The plots also demonstrate, once again, the non-Gaussian nature of these results.

The contour plots presented above may be of some use in helping to understand the uncertainty in a orbit decay prediction; however the main thing they show us is that the sensitivity to solar flux variation is a complex function of multiple variables. Figure 16 shows a 3-D surface of the percent uncertainty in orbit lifetime as a function of both initial altitude and re-entry date (years from solar minimum). This figure is perhaps the most interesting, in that it shows significantly increased sensitivity for spacecraft that re-enter during the years between solar max, and the next solar minimum. What this plot appears to show is something we may have predicted: that objects that "fly over" solar maximum and into the next cycle will have an increased sensitivity to flux variations, while those that do not survive the rising edge of the solar maximum will not.

CONCLUSIONS

In spite of considerable frustration resulting from an overabundance of poorly modeled parameters and processes in the orbit decay prediction problem, we continue to attempt to better understand the uncertainties in such predictions. As a result of this study, we add daily variations in solar flux to our list of variables requiring consideration. The results presented herein clearly demonstrate that our traditional flux modeling approach for orbit decay prediction, in which we (prior to this effort) considered only the monthly solar flux values as opposed to daily values, introduces additional uncertainty in our orbit lifetime predictions on the order of 5-40%. We observe that the greatest sensitivity occurs for those spacecraft on the cusp of flying over the solar maximum, while the least sensitivity occurs for objects re-entering during the rising edge of the solar cycle.

Perhaps the most important conclusion of this work is the following: in most cases, short-term flux variations *must* be included in orbit decay prediction to fully understand the errors associated with those predictions. This type of Monte-Carlo analysis is particularly

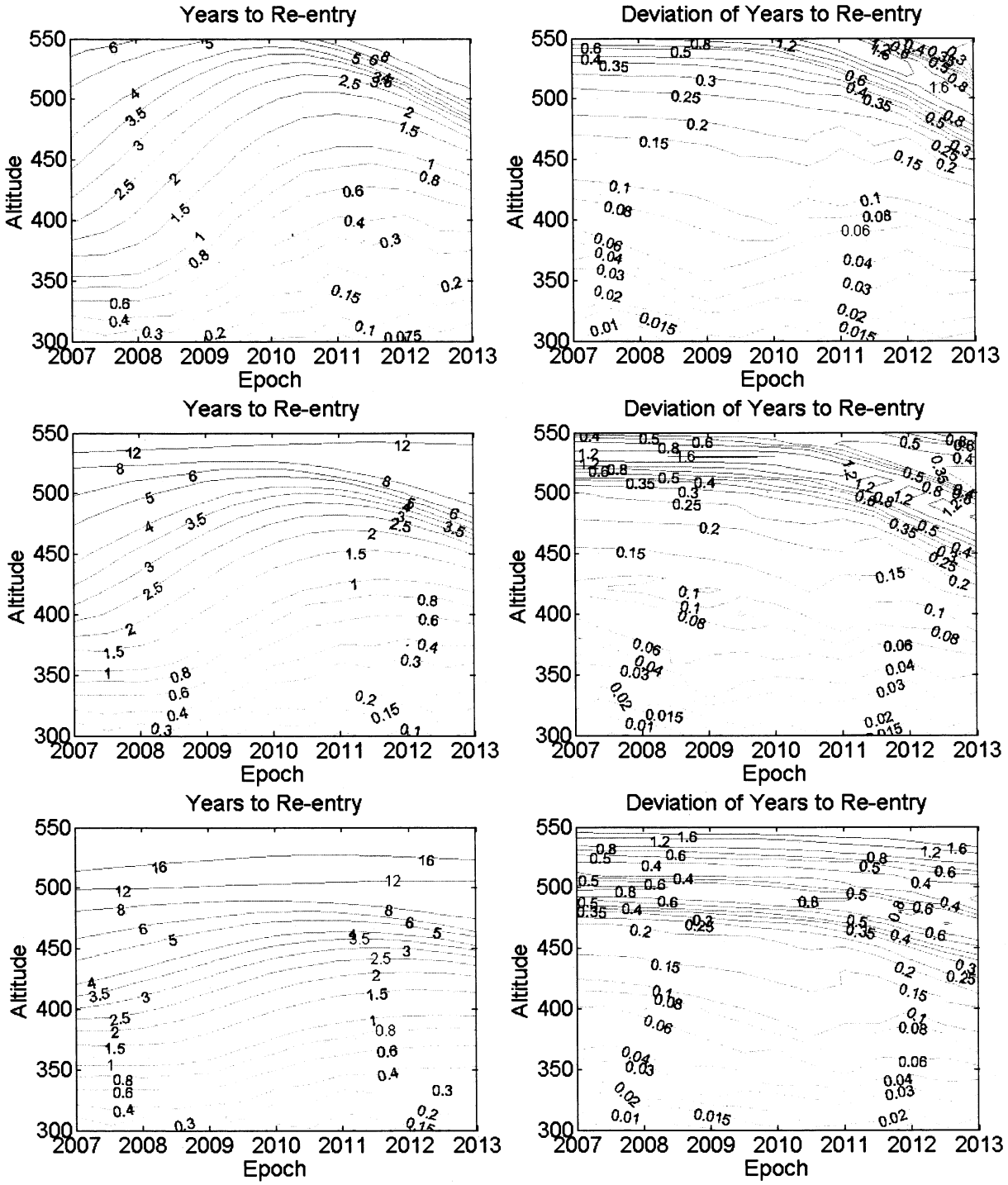

Figure 14: Orbit lifetime contours for multiple 100-flux-sample, equatorial inclination sets with varying initial altitude. From top to bottom, input flux profiles are big, medium, and little, respectively. The three plots on the left show orbit lifetime in years from epoch. Right plots show orbit lifetime 1-σ values.

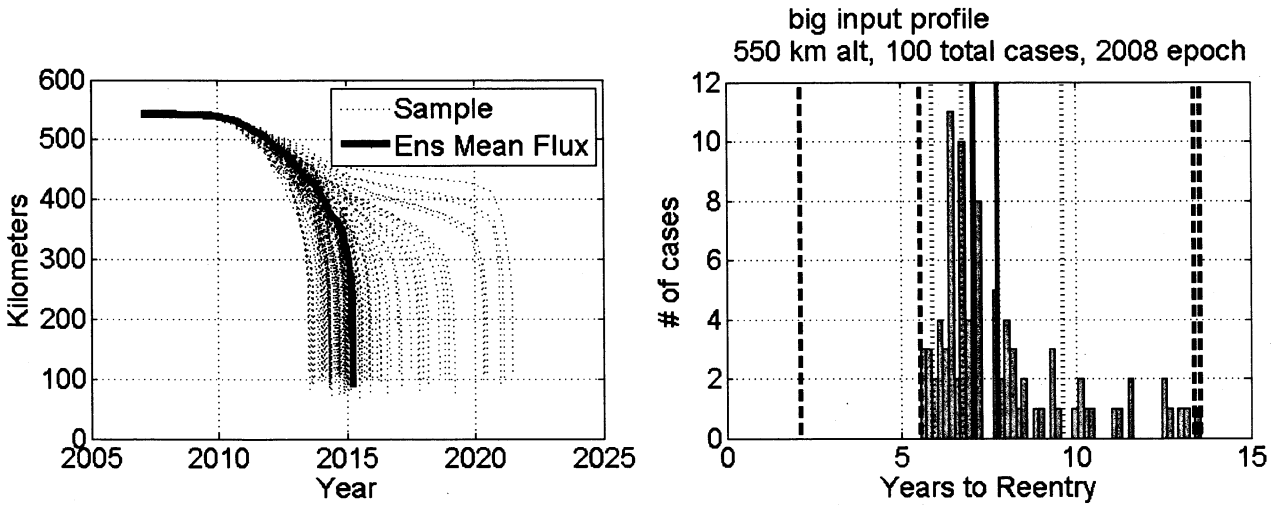

Figure 15: A highly sensitive sample, 550km initial altitude with epoch near solar minimum and a big flux input

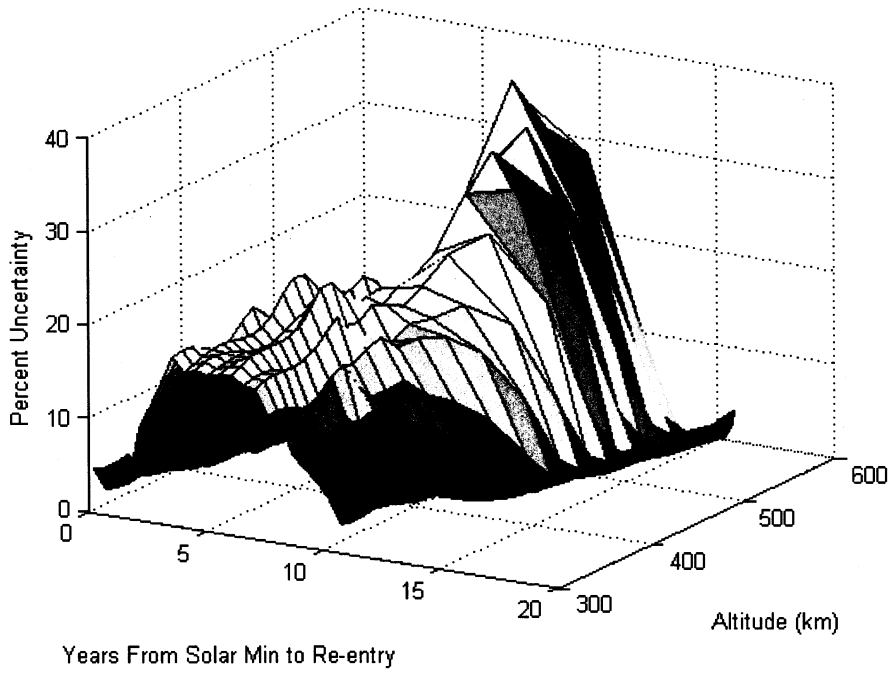

Figure 16: Orbit lifetime contours for multiple 100-flux-sample, equatorial inclination sets with varying initial altitude and big flux input

necessary given the non-Gaussian nature of the results, and the likely risk-sensitivity of spacecraft operators to one-in-a-million-type chance of an unexpected early re-entry.

We provide here the evidence of a new variable requiring consideration in this type of work. Clearly there are a number of significant variables remaining to be considered. We will leave them for future study.

REFERENCES

[1] Woodburn, J. and Lynch, S., "A Numerical Study of Orbit Lifetime," AIAA/AAS Astrodynamics Specialist Conference and Exhibit, Lake Tahoe, 2005, AAS 05-297.

[2] Schatten, K., "Fair Space Weather For Solar Cycle 24," Geophys. Res. Lett., 2005, 32, L21106-9.

[3] Schatten, K. and Pesnell, W. D., "Solar Cycle No. 24 and the Solar Dynamo," International Symposium on Space Flight Dynamics, Annapolis, Maryland, 2007, to be presented.

[4] Goddard Space Flight Center, "Flight Dynamics Facility Products Server," `https://wakata.nascom.nasa.gov/`, visited July 24, 2007.

[5] National Geophysical Data Center, "Selected Geomagnetic and Solar Activity Indices," `ftp://ftp.ngdc.noaa.gov/STP/GEOMAGNETIC_DATA/INDICES/KP_AP/`, visited July 24, 2007.

[6] Montenbruck, O. and Gill, E., Satellite Orbits – Models, Methods, and Applications, Springer Verlag, Heidelberg, Germany, 2000.

[7] Picone, J., Hedin, A. E., and Drob, D. P., "NRLMSISE-00 empirical model of the atmosphere: Statistical comparisons and scientific issues," Journal of Geophysical Research, Vol. 107, No. A12, 2002.

[8] Healy, L. M. and Akins, K. A., "Effects of solar activity level on orbit prediction using MSIS and Jacchia density models," AIAA/AAS Astrodynamics Specialist Conference and Exhibit, Providence, Rhode Island, 2004, AIAA 2004-4977.

[9] Akins, K. A., Healy, L. M., Coffey, S. L., and Picone, J. M., "Comparison of MSIS and Jacchia Atmospheric Density Models for Orbit Determination and Propagation," Advances in the Astronautical Sciences, Vol. 114, 2003, pp. 951–970, AAS 03-165.

[10] Hoyt, D. V. and Schatten, K. H., The Role of the Sun in Climate Change, Oxford Univ. Press, New York, 1997, Ch. 1.

[11] Tandberg-Hanssen, E., Solar Activity, Blaisdell Pub. Co., 1966, Ch. 2-5.

[12] White, O. R., The Solar Output and its Variations, Col. Assoc. Univ. Press, Boulder, 1977.

ACRONYMS AND ABBREVIATIONS

EIT Extreme ultraviolet Imaging Telescope

EPR Ephemeral Regions

EUV extreme ultraviolet

FDAB Flight Dynamics Analysis Branch

FDF Flight Dynamics Facility

GSFC Goddard Space Flight Center

MDI Michelson Doppler Imager

MSIS Mass Spectrometer Incoherent Scatter Radar

OD Orbit Determination

SOHO Solar and Heliospheric Observatory